



## Article

# A Comparative Analysis of High-Throughput and Conventional Phenotyping: Validation of Plantarray System and Dynamic Physiological Traits for Drought Tolerance in Watermelon

Rui Cheng <sup>1,2,3</sup>, Shiyu Zhao <sup>3</sup>, Xiaolong Shi <sup>3</sup>, Xin Liu <sup>2</sup>, Yan Tang <sup>3</sup>, Wenzhao Xu <sup>2</sup>, Binghua Xu <sup>2</sup>, Cong Jin <sup>3</sup>, Yudong Sun <sup>2,\*</sup> and Xuezheng Wang <sup>1,\*</sup>

<sup>1</sup> Key Laboratory of Biology and Genetic Improvement of Horticulture Crops (Northeast Region), Ministry of Agriculture and Rural Affairs, College of Horticulture and Landscape Architecture, Northeast Agricultural University, Harbin 150006, China; chengrui@jaas.ac.cn

<sup>2</sup> Huaiyin Institute of Agricultural Sciences of Xuhuai Region in Jiangsu, Huai'an 223001, China

<sup>3</sup> Huaiyin Institute of Technology, Huai'an 223003, China

\* Correspondence: sunyudong@jaas.ac.cn (Y.S.); wangxuezheng@neau.edu.cn (X.W.)

## Abstract

Drought stress is a major constraint on watermelon production worldwide. Conventional phenotyping methods for drought tolerance are often low-throughput and fail to capture dynamic physiological responses. This study validated the high-throughput phenotyping platform (Plantarray 3.0) against conventional methods by dynamically evaluating drought tolerance across 30 genetically diverse watermelon accessions. The Plantarray system quantified key dynamic traits, including transpiration rate (TR), transpiration maintenance ratio (TMR), and transpiration recovery ratios (TRRs), revealing distinct drought-response strategies. Principal component analysis (PCA) of these dynamic traits explained 96.4% of the total variance (PC1: 75.5%, PC2: 20.9%), clearly differentiating genotypes. A highly significant correlation ( $R = 0.941$ ,  $p < 0.001$ ) was found between the comprehensive drought tolerance rankings derived from Plantarray and conventional phenotyping. We identified five genotypes as highly tolerant and four as highly sensitive. The elite drought-tolerant germplasm, notably the wild species PI 537300 (*Citrullus colocynthis*) and the cultivated variety G42 (*Citrullus lanatus*), exhibited superior physiological performance and recovery capacity. The results demonstrate that the Plantarray system not only efficiently screens for drought tolerance but also provides deep insights into dynamic resistance mechanisms, offering a powerful tool and valuable genetic resources for breeding climate-resilient watermelon cultivars.

**Keywords:** drought resistance; comprehensive evaluation; Plantarray; watermelon



Academic Editor: Aušra Brazaitytė

Received: 9 October 2025

Revised: 10 November 2025

Accepted: 11 November 2025

Published: 14 November 2025

**Citation:** Cheng, R.; Zhao, S.; Shi, X.; Liu, X.; Tang, Y.; Xu, W.; Xu, B.; Jin, C.; Sun, Y.; Wang, X. A Comparative Analysis of High-Throughput and Conventional Phenotyping: Validation of Plantarray System and Dynamic Physiological Traits for Drought Tolerance in Watermelon. *Horticulturae* **2025**, *11*, 1374. <https://doi.org/10.3390/horticulturae11111374>

**Copyright:** © 2025 by the authors. Licensee MDPI, Basel, Switzerland. This article is an open access article distributed under the terms and conditions of the Creative Commons Attribution (CC BY) license (<https://creativecommons.org/licenses/by/4.0/>).

## 1. Introduction

Watermelon (*Citrullus lanatus*) is a globally significant horticultural crop, ranking among the top five most consumed fresh fruits worldwide, with a cultivation area of 3.48 million hectares (FAO 2024, available at: <https://www.fao.org/faostat/en/>, accessed on 22 August 2025). As the world's largest producer, China dominates both cultivation area and yield [1,2]. However, the expansion of watermelon production faces serious challenges due to limited arable land and increasing anthropogenic pressures. These constraints have pushed cultivation into marginal areas, where crops are frequently exposed to various abiotic stresses, including extreme temperatures and drought [3]. Although watermelon

originated in tropical Africa and has developed some adaptive mechanisms, it remains highly susceptible to drought stress [1–3]. This sensitivity presents a major constraint to production, as watermelon yield and quality are strongly dependent on adequate water supply, particularly during fruit development and ripening stages [4].

Globally, agriculture accounts for about 70% of freshwater withdrawals [5]. Drought is one of the most destructive meteorological disasters, and its impact is exacerbated by climate change. Rising global temperatures have increased evaporation rates, expanded arid regions, and intensified the agricultural constraints imposed by drought [6–8]. As a major abiotic stressor, drought severely impedes plant growth and development, often leading to substantial yield losses or even plant death [9,10]. In response, plants have evolved a suite of morphological and physio-biochemical adaptive mechanisms, collectively referred to as “drought resistance”, such as root system enhancement, reduced transpiration, and improved water use efficiency. Drought tolerance is a complex integrative trait that encompasses mechanisms including dehydration avoidance, dehydration tolerance, and recovery capacity [11]. Therefore, accurate phenotyping and evaluation of drought tolerance are crucial for identifying resistant germplasm resources.

Conventional methods for drought phenotyping, such as PEG-simulated drought, pot-based water withholding, and field-based natural drought screening [2], often rely on endpoint measurements of morphological and physiological parameters, including biomass, root architecture, photosynthetic rate, stomatal conductance, and survival rate [12,13]. While informative, these conventional methods are inherently limited. They are typically destructive, labor-intensive, and low-throughput. More critically, they only capture plant status at isolated time points, failing to resolve the dynamic physiological responses and acclimation processes that unfold throughout the drought period [14]. This temporal gap limits our ability to identify the key moments of stress onset, recovery capacity, and the underlying water-use strategies that define drought resistance mechanisms [15].

In contrast, high-throughput phenotyping (HTP) platforms, such as the Plantarray 3.0 system (Plant-DiTech, Rehovot, Israel), are designed to overcome these limitations. Unlike conventional endpoint measurements, this system functions as a network of precision weighing lysimeters that enable continuous, non-destructive, and simultaneous monitoring of whole-plant physiological traits—including transpiration rate, biomass accumulation, and water use efficiency—for the same plant throughout the experiment [16–18]. The core advantage lies in its temporal resolution and data integration. By measuring at 3 min intervals, it can capture diurnal patterns (e.g., midday stomatal closure) and transient stress responses that are completely missed by manual, single-time-point measurements. Furthermore, it automatically calculates integrative physiological indices that quantitatively describe a plant’s drought avoidance or tolerance strategy, providing a level of mechanistic insight that is difficult to achieve with conventional methods. The application of HTP for phenotyping horticultural crops (e.g., in drought stress studies) has advanced rapidly in recent years [18]. For instance, the Plantarray system has been reported in crops such as tomato [19], legumes [20], and barley [21]. However, its application in watermelon remains largely unreported to date.

In this study, the Plantarray 3.0 system was employed to monitor the physiological responses of 30 genetically diverse watermelon accessions under progressive drought stress, while conventional methods were used in parallel for validation. The system was effectively validated for its accuracy and efficiency in assessing drought tolerance in horticultural crops such as watermelon, and several drought-resistant watermelon germplasm materials were identified. This work lays a technical foundation for future applications of HTPs, including the Plantarray 3.0 system, in screening stress-resistant germplasm to support stress-resilience breeding.

## 2. Materials and Methods

### 2.1. Plant Materials

A diverse panel of 30 watermelon accessions was utilized in this study. This panel encompassed a broad genetic spectrum, representing four of the seven major *Citrullus* species: *C. colocynthis*, *C. amarus*, *C. mucosospermus*, and *C. lanatus*. The seeds, with origins spanning Asia, Africa, Europe, and North America, were provided by the Vegetable Research Center of the Huaiyin Institute of Agricultural Sciences of Xuhuai Region in Jiangsu and the Crop Breeding Platform of the Peking University Institute of Advanced Agricultural Sciences. The detailed passport information for all accessions is listed in Table 1.

**Table 1.** List of watermelon accessions used in the study.

No.	Accession	Species	Origin
1	PI 525081	<i>C. colocynthis</i>	Egypt
2	PI 632755	<i>C. colocynthis</i>	Namibia
3	PI 652554	<i>C. colocynthis</i>	India
4	PI 537300	<i>C. colocynthis</i>	Turkmenistan
5	PI 482276	<i>C. amarus</i>	Zimbabwe
6	PI 296341-FR	<i>C. amarus</i>	South Africa
7	PI 189225	<i>C. amarus</i>	Congo
8	RCAT 055816	<i>C. amarus</i>	Hungary
9	PI 532732	<i>C. mucosospermus</i>	Congo
10	PI 595203	<i>C. mucosospermus</i>	Nigeria
11	HeiShanRen	<i>C. lanatus landrace</i>	Ukraine
12	PI 381740	<i>C. lanatus landrace</i>	India
13	DaBanHongZiGua	<i>C. lanatus landrace</i>	China
14	PI 288522	<i>C. lanatus cultivar</i>	India
15	SanBaiGua	<i>C. lanatus landrace</i>	China
16	ShiHong No.2	<i>C. lanatus cultivar</i>	China
17	Sugarlee	<i>C. lanatus cultivar</i>	United States
18	Charleston Gray	<i>C. lanatus cultivar</i>	United States
19	Calhoun Gray	<i>C. lanatus cultivar</i>	United States
20	Allsugar	<i>C. lanatus cultivar</i>	United States
21	G42	<i>C. lanatus cultivar</i>	China
22	PKR6	<i>C. lanatus cultivar</i>	China
23	1908WME018	<i>C. lanatus cultivar</i>	China
24	1402WME016	<i>C. lanatus cultivar</i>	Japan
25	G48	<i>C. lanatus cultivar</i>	China
26	G38	<i>C. lanatus cultivar</i>	China
27	SSDL	<i>C. lanatus cultivar</i>	United States
28	G35	<i>C. lanatus cultivar</i>	Japan
29	1410WME023	<i>C. lanatus cultivar</i>	China
30	PI 612459	<i>C. lanatus cultivar</i>	Korea

### 2.2. Experimental Design and Growth Conditions

The experiment was conducted in a glass greenhouse in Huai'an, China (33.62° N, 119.02° E). The greenhouse dimensions were 20 m (length) × 8 m (width) × 5 m (height). Environmental control systems, including ground-source heat pumps, central air conditioning, heating (activated at <20 °C), cooling (activated at >35 °C), ventilation, and shading, were employed to maintain stable conditions. Throughout the experimental period, the ambient temperature and relative humidity (RH) inside the greenhouse were continuously monitored and recorded at 3 min intervals using a WatchDog2400 data logger (SPECTRUM Technologies Inc., Plainfield, IL, USA). These logged data confirmed that stable conditions were maintained, with an average daytime temperature of 34 ± 5 °C and RH of 50 ± 10%,

and a nighttime temperature of  $24 \pm 5 \text{ }^\circ\text{C}$  with RH of  $80 \pm 10\%$  (Figure 1B). The natural daily fluctuations in air temperature ( $T_{\text{air}}$ ), photosynthetically active radiation (PAR), relative humidity (RH), and vapor pressure deficit (VPD) were also presented in Figure 1B. The raw environmental data logged at 3-min intervals are provided in Supplementary Table S1.

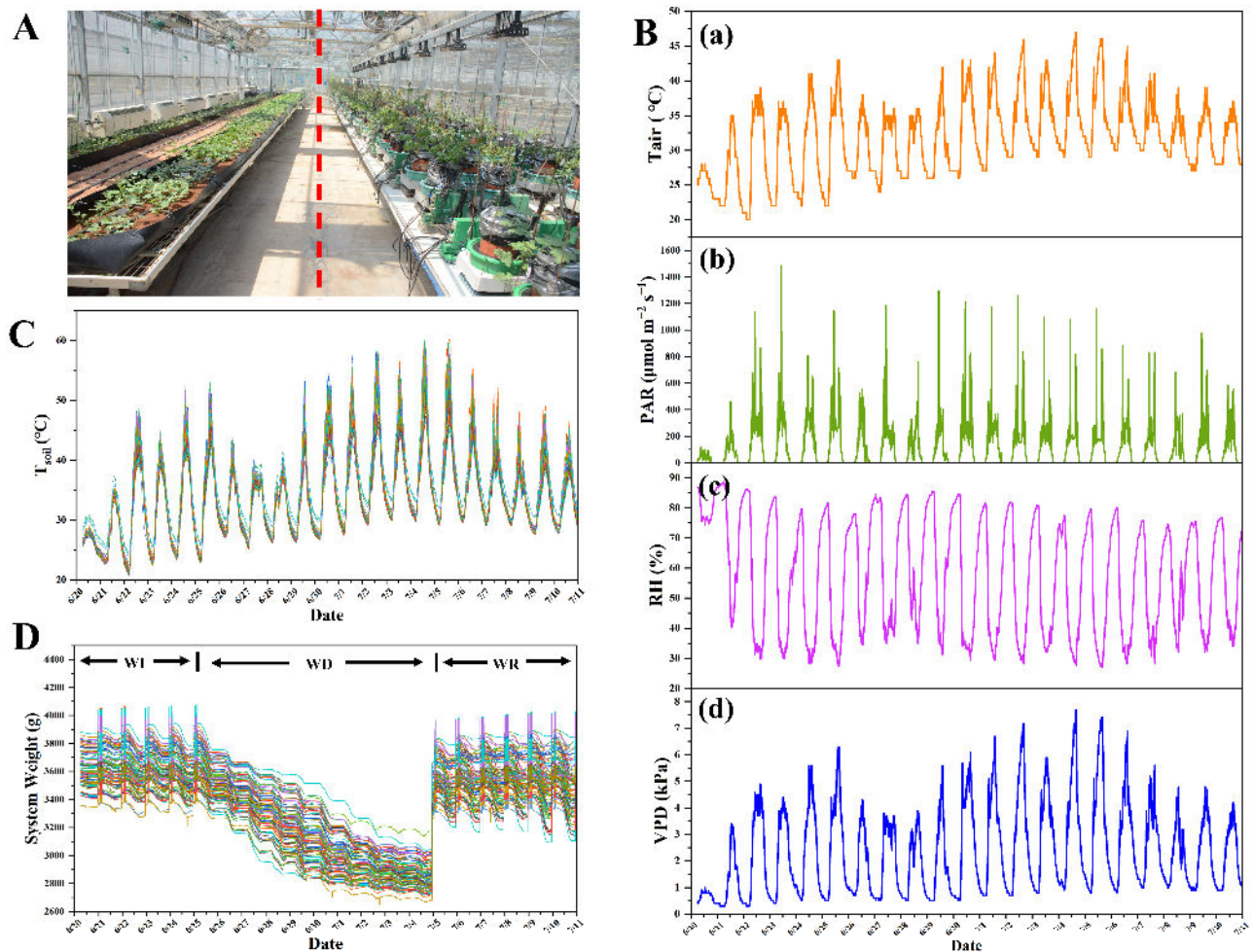


**Figure 1.** Environmental conditions and experimental setup for the drought phenotyping experiment. (A) Schematic of the two parallel phenotyping approaches: the traditional method with manual irrigation (left) and the high-throughput, automated Plantarray 3.0 system (right). All plants across both systems were of identical age and genetic material (30 watermelon varieties). (B) Dynamics of key meteorological parameters during the experimental period: air temperature ( $T_{\text{air}}$ , (a)), photosynthetically active radiation (PAR, (b)), relative humidity (RH, (c)), and vapor pressure deficit (VPD, (d)). (C) Dynamics of soil temperature ( $T_{\text{soil}}$ ). Colors represent different individual units in the Plantarray system. (D) Dynamics of the total pot weight throughout the experiment. Colors represent different individual units in the Plantarray system. The experimental timeline is divided into well-irrigated (WI), progressive water deficit (WD), and water recovery (WR) phases.

For each watermelon accession, 24 plump seeds were surface-sterilized, wrapped in moist germination towels, and incubated at  $30 \text{ }^\circ\text{C}$  in a constant-temperature incubator. Germinated seeds were sown in 72-cell trays filled with a PINDSTRUP SUBSTRATE peat moss (Pindstrup Mosebrug A/S, Ryomgård, Denmark) and covered with a thin layer of vermiculite. Seedlings were irrigated with a 2‰ ( $w/v$ ) solution of “Zhonghua Yangtian” series compound fertilizer (20-20-20 + Microelements, Sinofert, Yantai, China). The nutrient solution provided the following final concentrations: 28.6 mM N, 5.6 mM P, 8.5 mM K, 0.17 mM Mg, 1.8  $\mu\text{M}$  Fe, 9.2  $\mu\text{M}$  Zn, 1.2  $\mu\text{M}$  B, 0.7  $\mu\text{M}$  Mn, 0.16  $\mu\text{M}$  Cu, and 0.10  $\mu\text{M}$  Mo.

This treatment continued until the seedlings reached the three-leaf stage, at which point they were transplanted.

Each seedling was transplanted into an individual pot (16 cm × 13 cm × 18 cm, 1.5 L volume) filled with Profile Porous Ceramic (PPC) substrate (Profile Products LLC, Buffalo Grove, IL, USA). The PPC substrate, a kiln-fired porous ceramic, had the following characteristics: particle diameter ≈ 0.2 mm, pH 5.5 ± 1, porosity 74%, and cation exchange capacity (CEC) of 33.6 mEq/100 g. The field capacity of the PPC substrate in pot culture, determined gravimetrically, was 54.9% on average.

### 2.3. Drought Stress Treatments and Phenotyping Platforms

At the five-leaf stage, seedlings of each genotype were subjected to drought phenotyping using two parallel approaches (Figure 1A), and the detailed layout within the Plantarray system is provided in Supplementary Table S2.

**High-throughput Physiological Phenotyping Platform (Plantarray 3.0):** The Plantarray system (Plant-DiTech, Rehovot, Israel) was employed, which integrates gravimetric units, soil and atmospheric sensors, a controller, and an automated irrigation system for continuous, simultaneous monitoring of plant weight, physiological responses, and soil/atmospheric parameters [16–18]. Seedlings were arranged on the platform in a completely randomized design, with three or four independent plants per genotype.

**Traditional Water-Withholding Method:** A parallel pot-based experiment was conducted under the same greenhouse conditions to serve as a control and for validation. This setup included two distinct treatment groups, Drought Stress (DS) Group: subjected to water withholding, with three independent biological replicates per genotype, and Well-Watered (WW) Control Group: Maintained under normal irrigation, with three independent biological replicates per genotype.

All plants from both the Plantarray system and the traditional DS group were subjected to drought stress simultaneously. The experiment comprised three consecutive phases:

**Well-Irrigated (WI) Phase (7 days, 20/6–26/6):** All plants were maintained under optimal irrigation. In the Plantarray system, irrigation was automatically triggered four times daily (at 23:00, 01:00, 02:00, and 03:00), each time delivering the “Zhonghua Yangtian” series nutrient solution (for 240 s, until supersaturation). As detailed in Section 2.2, this solution provided a balanced nutrient supply. In contrast, plants in the traditional experiment were manually irrigated between 07:00 and 09:00 each morning.

**Progressive Water Deficit (WD) Phase (8 days, 27/6–4/7):** To induce drought stress, irrigation was completely and simultaneously withheld for all plants on the Plantarray platform and all plants in the traditional DS group. Throughout this phase, the WW control group in the traditional experiment continued to receive daily manual irrigation. The onset of drought stress was confirmed by a continuous decline in the total pot weight as recorded by the Plantarray system (Figure 1D, Table S3). Plant physiological indicators in the traditional experiment were measured manually at the end of this phase.

**Water Recovery (WR) Phase (8 days, 5/7–12/7):** Full irrigation was resumed for all drought-stressed plants according to the WI phase schedule to assess their recovery capacity.

### 2.4. Data Acquisition and Measurements

#### 2.4.1. Automated Physiological Phenotyping

The Plantarray system, a high-precision, high-throughput gravimetric lysimeter platform equipped with load cells, 5TM soil sensors, and WatchDog2400 atmospheric monitoring sensors, continuously recorded data at 3 min intervals [17]. The system automatically recorded and calculated the following parameters [16–18]: system weight (g) per

pot, soil volumetric water content (VWC,  $\text{m}^3 \cdot \text{m}^{-3}$ ), air temperature ( $T_{\text{air}}$ ,  $^{\circ}\text{C}$ ), relative humidity (RH, %), and photosynthetically active radiation (PAR,  $\mu\text{mol} \cdot \text{m}^{-2} \cdot \text{s}^{-1}$ ). From these primary data, the vapor pressure deficit (VPD, kPa) was calculated. Furthermore, a suite of physiological parameters was automatically derived using the integrated SPAC (<https://spac.plant-ditech.com>, accessed on 22 August 2025) analytics software, including but not limited to daily plant growth (PG,  $\text{g} \cdot \text{DW} \cdot \text{d}^{-1}$ ), whole-plant transpiration rate (TR,  $\text{g} \cdot \text{min}^{-1}$ ), and water use efficiency (WUE). To reveal intrinsic plant physiological responses, the transpiration rate was normalized by VPD for subsequent analyses. The detailed methodologies align with our previous work [22].

#### 2.4.2. Drought Injury Index

At the end of the WD phase, visual drought injury symptoms were scored for all plants based on a standardized scale. The Drought Injury Index (DII) was calculated for each genotype as follows [23]:

$$\text{DII} = (0 \times N_0 + 1 \times N_1 + 2 \times N_2 + 3 \times N_3 + 4 \times N_4) / N_{\text{total}} \quad (1)$$

where  $N_0$  to  $N_4$  represent the number of plants in each damage severity class (0–4, from no symptoms to plant death. The detailed classes were as follows: 0 (No symptoms, plant grows normally with erect stem and fully expanded leaves); 1 (Erect stem with drooping leaves or leaf margin rolling); 2 (Erect stem but with shriveled epidermis and severely drooping leaves); 3 (Stem bends due to water loss, and all leaves droop); 4 (Seedling stem bends, leaves droop, and leaf margins desiccate, indicating plant death), and  $N_{\text{total}}$  is the total number of plants [23]. A higher DII indicates poorer drought tolerance.

#### 2.4.3. Photosynthetic Parameter and Growth Index

At the end of the WD phase in a traditional water-withholding experiment, destructive sampling and measurements were conducted. Three representative seedlings per genotype from both the DS and WW groups were randomly selected for analyses of photosynthesis and growth. Photosynthetic parameters were measured between 9:00 and 12:00 h on the mature, fully expanded leaves using a portable photosynthesis system (LCpro T, ADC BioScientific, Hoddesdon, UK). The measurements were conducted under controlled conditions: leaf chamber irradiance was set to a saturating photosynthetic photon flux density using the instrument's internal red-blue light source, and the  $\text{CO}_2$  concentration in the Cref was maintained at  $420 \mu\text{mol} \cdot \text{mol}^{-1}$ . Under steady-state conditions, the net photosynthetic rate ( $A$ ,  $\mu\text{mol} \text{CO}_2 \cdot \text{m}^{-2} \cdot \text{s}^{-1}$ ), intercellular  $\text{CO}_2$  concentration ( $C_i$ ,  $\mu\text{mol} \cdot \text{mol}^{-1}$ ), stomatal conductance ( $g_s$ ,  $\text{mol} \text{H}_2\text{O} \cdot \text{m}^{-2} \cdot \text{s}^{-1}$ ), and leaf transpiration rate ( $E$ ,  $\text{mmol} \text{H}_2\text{O} \cdot \text{m}^{-2} \cdot \text{s}^{-1}$ ) were recorded.

Subsequently, plants were separated into shoots and roots at the cotyledonary node. The following growth parameters were measured: vine length (VL, cm) and root length (RL, cm) were measured using a standard ruler. For fresh weight determinations, shoot fresh weight (SFW, g) and root fresh weight (RFW, g) were measured with an analytical balance. For root fresh weight determination, roots were carefully washed to remove substrate, and surface moisture was gently blotted dry. All samples were then oven-dried: enzyme deactivation was performed at  $105^{\circ}\text{C}$  for 30 min, followed by drying at  $70^{\circ}\text{C}$  until a constant weight (i.e., less than 0.1% change over a 2 h interval) was achieved to determine shoot dry weight (SDW, g) and root dry weight (RDW, g). The root-to-shoot ratio (RSR) was subsequently calculated as  $\text{RDW}/\text{SDW}$ .

## 2.5. Comprehensive Evaluation of Drought Tolerance

### 2.5.1. Dynamic Phenotyping Indices from Plantarray

Based on the continuous data from the Plantarray system, four key indices were calculated for each genotype to quantify different aspects of drought response [24]:

Transpiration Maintenance Ratio (TMR):

$$\text{TMR} = \text{Mean\_TR(WD)}/\text{Mean\_TR(WI)} \quad (2)$$

Reflects the ability to maintain transpiration under mild-to-moderate stress.

Cumulative Transpiration Ratio (CTR):

$$\text{CTR} = \text{Total\_Tr(WD)}/\text{Total\_Tr(WI)} \quad (3)$$

Serves as a proxy for biomass production maintenance under stress.

Water Use Efficiency Increase Ratio (WUEI):

$$\text{WUEI} = \text{WUE(WD)}/\text{WUE(WI)} \quad (4)$$

Indicates the improvement in instantaneous water use efficiency under stress.

Transpiration Recovery Ratio (TRR):

$$\text{TRR} = \text{Mean\_TR(WR)}/\text{Mean\_TR(WI)} \quad (5)$$

Assesses the capacity to recover transpiration upon rehydration.

### 2.5.2. Drought Tolerance Coefficients from Conventional Measurements

For the traditional water-withholding experiment, the drought tolerance coefficient (DTC) was calculated for each measured morphological and physiological trait as [25]:

$$\text{DTC} = \text{Value\_DS}/\text{Value\_WW} \quad (6)$$

where Value\_DS and Value\_WW represent the mean values under DS and WW conditions, respectively. The inverse of the Drought Injury Index (DII\_inv) was used as a positive indicator of survival.

### 2.5.3. Principal Component Analysis and Comprehensive D-Value Calculation

To integrate multiple physiological indices into a robust assessment of drought tolerance, we employed a principal component analysis (PCA) followed by a membership function evaluation [26,27]. PCA was performed separately on the Plantarray-derived indices matrix and the conventional DTCs matrix using the *prcomp* function in R. Prior to PCA, all variables were scaled and centered (Z-score standardization). The suitability for PCA was confirmed with the Kaiser–Meyer–Olkin (KMO) measure using the *psych* package (v2.3.6), where a KMO overall value > 0.6 was considered acceptable, and Bartlett’s test of sphericity using the *psych* package ( $p < 0.001$ ).

Principal Components (PCs) with eigenvalues greater than 1 (Kaiser’s criterion) were retained. The comprehensive drought tolerance value (D-value) was computed using a membership function method [27,28]:

First, the membership function value  $U(X_j)$  for the score of the  $j$ -th PC was calculated to normalize the scores to a range of:

$$U(X_j) = (X_j - X_{\min})/(X_{\max} - X_{\min}) \quad (7)$$

where  $X_j$  is the score of a genotype corresponding to the  $j$ -th PC, and  $X_{max}$  and  $X_{min}$  are the maximum and minimum scores on that PC, respectively.

Second, the weight ( $W_j$ ) of each PC was determined by its contribution rate to the total variance:

$$W_j = P_j / \sum P_j \quad (j = 1, 2, \dots, n) \quad (8)$$

where  $P_j$  is the contribution rate of the  $j$ -th PC.

Finally, the D-value was computed as:

$$D = \sum [U(X_j) \times W_j] \quad (j = 1, 2, \dots, n) \quad (9)$$

This approach effectively synthesizes information from multiple correlated traits into a single, unified metric. Genotypes were ranked based on their D-values, with a higher D-value indicating superior comprehensive drought tolerance.

#### 2.5.4. Cluster Analysis for Drought Response Typing

To identify distinct drought response profiles, k-means clustering was performed using the `kmeans` function in R to classify genotypes into distinct drought response groups based on their comprehensive D-values [2]. The optimal number of clusters was determined by evaluating  $k$  values from 2 to 5 using the elbow method (via `fviz_nbclust` in the *factoextra* package) and by maximizing the average silhouette width (via `silhouette` in the *cluster* package).

#### 2.6. Statistical Analysis

Data collation was performed using Microsoft Excel 2019. Statistical analyses and graphical presentation were performed using the student version of Origin 2022 software (OriginLab Corporation, Northampton, MA, USA) and R software (version 4.3.0). The following R packages were employed: *lme4* (version 1.1-34) for linear mixed models (LMMs), *lmerTest* (version 3.1-3) for obtaining  $p$ -values from LMMs, *emmeans* (version 1.10.0) for post hoc comparisons and effect size estimation, *factoextra* for PCA, *ggcorrplot* (v0.1.4) for correlation matrices, *psych* for descriptive statistics and *ggplot2* (version 3.4.4) for data visualization. A significance level of  $p < 0.05$  was applied for all statistical tests.

### 3. Results

#### 3.1. Phenotypic Variation in Response to Drought Stress

At the end of the WD phase, all 30 watermelon accessions exhibited visible drought injury symptoms; however, the severity of damage varied profoundly across the diverse panel (Table 2). The DII quantified this variation, revealing a wide spectrum of phenotypic responses. The DII, assessed for plants on the Plantarray 3.0 system, ranged from 0 (no visible symptoms) in the most tolerant accessions to 4.0 (plant death) in the most sensitive ones, with a mean value of 2.08 (Tables 2 and S4). A highly consistent trend was observed in the traditional pot-based experiment, where DII values also spanned from 0 to 4.0, affirming the robustness of the visual assessment (Table S5).

A clear interspecific trend was evident upon examining the DII data. Wild relatives, particularly accessions from *C. colocynthis* and *C. amarus*, generally exhibited superior drought tolerance. For instance, PI 537300 (*C. colocynthis*), PI 652554 (*C. colocynthis*), and PI 482276 (*C. amarus*) displayed only mild to moderate damage ( $DII \leq 1.0$ ). In stark contrast, modern cultivated varieties (*C. lanatus* cultivars) were predominantly among the most drought-sensitive materials, such as ShiHong No.2, Sugarlee, and Charleston Gray, which reached the maximum DII value of 4.0, indicating plant death, while others like G38 and SSDL also showed high susceptibility ( $DII \geq 3.75$ ). Notably, exceptions existed within

both groups, as exemplified by the cultivated variety G42, which demonstrated remarkable tolerance, underscoring the potential for identifying novel sources of drought tolerance within cultivated germplasm.

**Table 2.** Variation in drought injury index (DII) and dynamic physiological indices among 30 watermelon accessions under drought stress.

Accession	DII (Plantarray)	DII (Traditional)	TMR	CTR	WUEI	TRR
PI 525081	2.67	2.33	0.31	0.41	0.40	0.49
PI 632755	2.25	1.89	0.33	0.44	0.46	0.80
PI 652554	1.00	1.14	0.40	0.53	0.58	0.58
PI 537300	0.00	0.00	0.48	0.63	0.64	1.22
PI 482276	1.00	1.33	0.42	0.55	0.68	0.67
PI 296341-FR	3.75	4.00	0.25	0.33	0.37	0.83
PI 189225	0.5	1.11	0.43	0.58	0.66	0.56
RCAT055816	1.33	1.67	0.34	0.45	0.60	0.79
PI 532732	1.25	1.33	0.36	0.48	0.68	1.21
PI 595203	1.33	1.56	0.36	0.48	0.61	0.49
HeiShanRen	0.00	0.89	0.44	0.59	0.71	0.54
PI 381740	3.00	2.11	0.27	0.36	0.49	0.68
DaBanHongZiGua	1.5	1.67	0.34	0.45	0.52	0.89
PI 288522	2.25	2.00	0.32	0.43	0.56	0.86
SanBaiGua	3.00	2.89	0.26	0.34	0.38	0.67
ShiHongNo.2	4.00	3.89	0.23	0.30	0.27	0.48
Sugarlee	4.00	4.00	0.25	0.33	0.33	0.64
CharlestonGray	4.00	4.00	0.23	0.30	0.35	0.45
CalhounGray	2.75	2.50	0.27	0.37	0.52	0.89
Allsugar	2.75	2.56	0.28	0.37	0.46	0.51
G42	0.00	0.33	0.44	0.58	0.73	0.76
PKR6	2.67	1.89	0.29	0.39	0.46	0.48
1908WME018	0.33	1.00	0.42	0.56	0.76	0.95
1402WME016	2.75	2.50	0.30	0.40	0.38	0.60
G48	2.33	2.11	0.32	0.43	0.43	0.50
G38	3.00	3.67	0.28	0.37	0.41	0.42
SSDL	3.75	2.57	0.25	0.34	0.39	0.82
G35	1.5	1.67	0.34	0.45	0.56	0.47
1410WME023	1.75	2.00	0.33	0.44	0.56	0.78
PI 612459	1.33	1.89	0.36	0.48	0.48	0.46
Mean	2.08	2.11	0.33	0.44	0.51	0.68
SD	1.29	1.10	0.07	0.09	0.13	0.21
Min	0.00	0.00	0.23	0.30	0.27	0.42
Max	4.00	4.00	0.48	0.63	0.76	1.22
CV	62.02	52.13	21.10	21.10	25.50	31.40

### 3.2. The Plantarray System Reveals Dynamic Physiological Responses to Progressive Drought Stress

The Plantarray 3.0 system captured detailed physiological dynamics throughout the drought-recovery cycle. Initial examination of the raw TR data showed strong diurnal fluctuations, which were primarily driven by ambient environmental conditions (Figure 2A, Table S6). To delineate intrinsic plant physiological activity from the effects of the environment, we normalized TR by the VPD [22]. This normalization revealed a clear and physiologically meaningful response pattern (Figure 2B). The TR/VPD displayed sustained high rates during the WI phase, a rapid decline after irrigation was withheld, a significant decrease to the lowest level as the drought intensified, and a partial recovery upon rewater-

ing. Concurrently, the substrate VWC decreased continuously during the WD phase and was fully reversed during the WR phase (Figure 2C, Table S7).

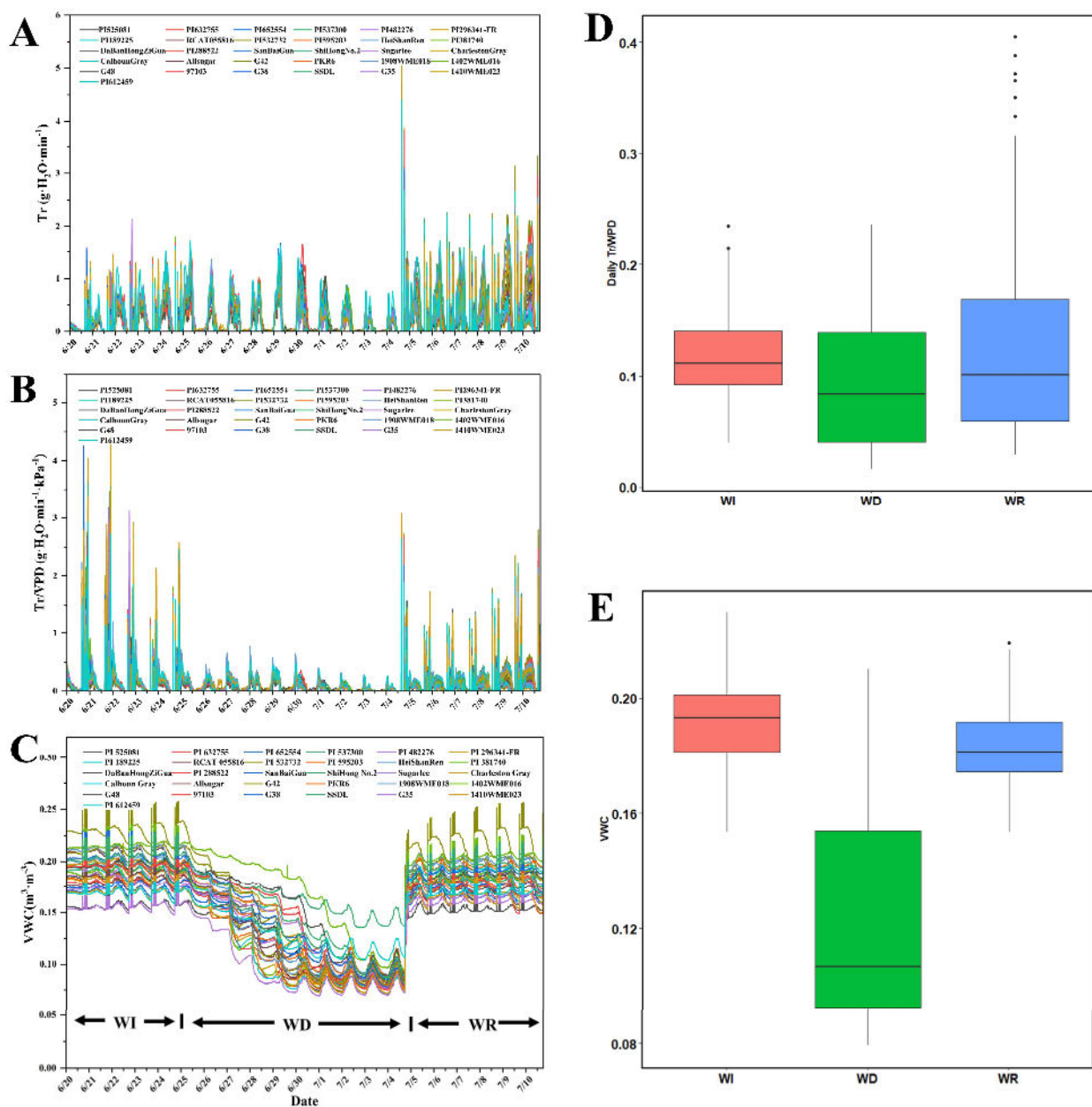


**Figure 2.** Dynamic physiological responses of watermelon accessions to drought stress and recovery, as monitored by the Plantarray system. (A) Diurnal patterns of TR for all accessions throughout the experimental course. (B) Dynamics of the VPD-normalized TR (C) Changes in substrate VWC for all accessions. (D) Boxplots of TR aggregated for the WI, WD, and WR phases. (E) Boxplots of substrate VWC aggregated for the WI, WD, and WR phases. The box represents the interquartile range (IQR), and the horizontal line inside the box denotes the median.

Guided by previous findings from our laboratory on the utility of TR and VWC dynamics for assessing plant water sensitivity, we computed a suite of parameters: TMR, CTR, WUEI, and TRR from these measurements to comprehensively evaluate drought tolerance in watermelon (Table 2). The TMR and CTR, which reflect plant water use under increasing stress, varied approximately two-fold across the panel, with ranges of 0.226–0.475 and 0.301–0.633, respectively. The capacity to recover transpiration after stress, measured by the TRR, also differed markedly, with values ranging from 0.420 to 1.216. Notably, several

accessions, including PI 537300 (*C. colocynthis*) and PI 532732 (*C. mucosospermus*), exhibited TRR values exceeding 1.0, indicating a full recovery to pre-stress transpiration levels. Furthermore, the WUEI varied from 0.266 to 0.763, demonstrating divergent strategies in optimizing carbon gain relative to water loss during drought. Statistical aggregation of the data confirmed the physiological shifts between phases. The distribution of daily Tr was high and narrow during WI, shifted to significantly lower and more variable values during WD, and showed an intermediate median with broad variability during WR (Figure 2D). This pattern is consistent with the wide ranges observed for TMR, CTR, and TRR in Table 2. Similarly, VWC was stable and high during WI and WR but showed a sharp, uniform decline during WD (Figure 2E), confirming the effectiveness of the drought treatment.

### 3.3. High-Throughput Phenotyping Enables the Identification of Contrasting Drought Response Patterns

To decipher the interrelationships among the dynamic physiological traits and to comprehensively evaluate drought tolerance, we performed an integrated analysis of TMR, CTR, WUEI, and TRR. Correlation analysis revealed a strong positive association between TMR, CTR, and WUEI ( $r > 0.88$ ,  $p < 0.001$ ), indicating that accessions which maintained higher transpiration under stress also tended to exhibit higher water use efficiency (Figure 3A). In contrast, the TRR showed only weak to moderate correlations with the other three indices ( $r < 0.42$ ), suggesting that the capacity for post-drought recovery is a relatively independent component of the overall drought response strategy. PCA further confirmed this trait dissociation (Figure 3B), as the first two PCs effectively captured the variance among accessions. PC1 (75.5%), which accounted for the majority of the variance, was strongly and positively loaded by TMR, CTR, and WUEI. However, TRR was the primary driver of PC2 (20.9%), forming a distinct vector separated from the other traits. The D-value was subsequently derived by integrating the PCs with membership function analysis, establishing a robust ranking of the 30 accessions (Figure 3C). The D-values exhibited a continuous distribution, with PI 537300 (*C. colocynthis*), G42 (*C. lanatus cultivar*), and HeiShanRen (*C. lanatus lan-drace*) identified as the top three most drought-tolerant genotypes. Conversely, modern cultivars such as ShiHong No.2 (*C. lanatus cultivar*), Charleston Gray (*C. lanatus cultivar*), and Sugarlee (*C. lanatus cultivar*) ranked as the most sensitive. The relationship between each accession and the physiological traits was explicitly visualized through a clustering heatmap (Figure 3D). The heatmap revealed more complex strategies; for instance, PI 532732 (*C. mucosospermus*) displayed an exceptional recovery profile (high TRR) coupled with moderate maintenance, while PI 296341-FR (*C. amarus*) showed poor maintenance but intermediate recovery, illustrating the distinct drought response patterns captured by the high-throughput phenotyping. Hierarchical cluster analysis classified the accessions into three distinct groups: drought-tolerant (e.g., G42, PI 537300), intermediate (e.g., G35, PI 595203), and sensitive (e.g., G48, Sugarlee), effectively stratifying the germplasm based on integrated physiological strategies (Figure 3E).

### 3.4. Post-Stress Physiological and Morphological Alterations Measured by Traditional Methods

In parallel with the high-throughput phenotyping for drought tolerance evaluation in watermelon, we measured key photosynthetic and morphological traits using traditional methods at the drought endpoint, the calculated DTCs for each trait and accession are summarized in Table 3, and all raw data are provided in Tables S8 and S9. Across the germplasm, drought stress significantly inhibited most photosynthetic parameters. The DTC for net photosynthetic rate (DTC\_A) was reduced by approximately 40% on average, with values ranging from 0.14 (SanBaiGua) to 1.37 (PI 381740). The DTCs for stomatal conductance (DTC\_gs) and leaf transpiration rate (DTC\_E) also showed substantial declines. In contrast, the DTC for intercellular CO<sub>2</sub> concentration (DTC\_ci) increased under

drought in the majority of accessions. Morphological traits exhibited distinct responses to water deficit. Above-ground growth was consistently more suppressed than below-ground growth (Table 3). The DTC for main vine length (DTC\_VL) and shoot dry weight (DTC\_SDW) were reduced to 59% and 70% of their well-watered controls, on average. In comparison, the DTC for primary root length (DTC\_RL) was less affected, and the DTC for root dry weight (DTC\_RDW) showed an average increase. This differential inhibition of shoot versus root growth resulted in a marked increase in the DTC for root-to-shoot ratio (DTC\_RSR), with individual values varying widely from 0.34 (Sugarlee) to 9.14 (G42).

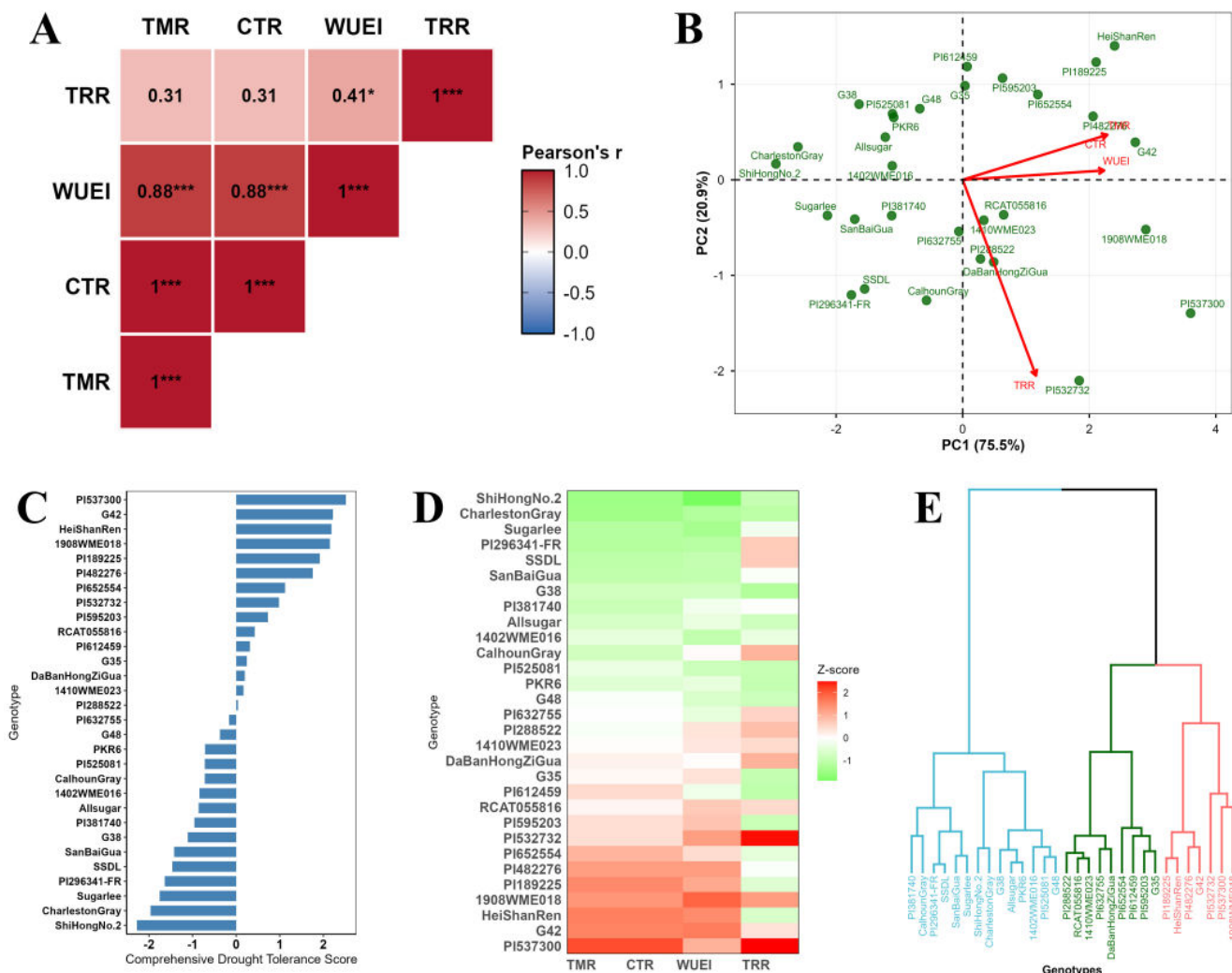


**Figure 3.** Identification of drought response patterns and comprehensive tolerance evaluation in watermelon germplasm by Plantarray system. (A) Correlation matrix of TMR, CTR, WUEI, and TRR. Values in cells represent Pearson’s correlation coefficients (r) with significance levels indicated as \*  $p < 0.05$ , \*\*\*  $p < 0.001$ . (B) PCA biplot showing accessions (dots) and trait vectors (arrow). The percentages of variance explained by the first and second principal components (PC1 and PC2) are 75.5% and 20.9%, respectively. (C) Drought tolerance ranking based on the D-value derived from PCA and membership function analysis. (D) Clustered heatmap of Z-score normalized values for the four physiological indices across all accessions. (E) Hierarchical clustering dendrogram classifying the 30 accessions into three distinct groups: drought-tolerant (red), intermediate (green), and sensitive (blue), based on their integrated physiological strategies.

**Table 3.** Drought tolerance coefficients (DTCs) of photosynthetic parameters and growth traits for 30 watermelon accessions subjected to drought stress.

Sample	Photosynthetic Parameters						Growth Traits				
	DTC_A	DTC_gs	DTC_E	DTC_ci	DTC_RL	DTC_VL	DTC_SFW	DTC_SDW	DTC_RFW	DTC_RDW	DTC_RSR
HeiShanRen	0.46	0.31	0.38	1.46	0.91	0.84	0.62	0.84	3.11	2.50	2.98
PI296341-FR	0.79	0.93	1.00	1.35	1.34	0.32	0.31	0.16	0.89	1.33	8.36
SSDL	1.17	0.85	0.96	1.41	1.46	0.53	0.40	0.49	1.71	2.00	4.06
G35	0.25	0.33	0.36	1.08	1.60	0.68	0.38	0.55	1.33	1.33	2.41
PI632755	0.79	0.53	0.60	1.46	1.33	0.46	0.28	0.43	1.23	2.00	4.69
PI595203	0.62	0.21	0.27	1.61	1.26	0.54	0.51	0.77	1.17	1.77	2.30
PI652554	0.33	0.33	0.44	1.38	1.48	0.63	0.45	0.54	1.93	3.00	5.52
1908WME018	0.55	0.25	0.29	1.51	1.11	1.02	0.63	1.07	1.95	1.60	1.50
PI482276	0.57	0.31	0.37	1.50	0.77	1.15	0.77	0.89	1.17	1.70	1.91
PKR6	0.44	0.53	0.70	1.61	0.88	0.56	0.47	0.49	1.60	2.20	4.51
PI189225	0.53	0.29	0.32	1.40	1.39	0.77	0.55	0.70	2.20	2.58	3.69
RCAT055816	0.66	0.45	0.50	1.44	1.62	0.77	0.59	0.87	1.47	2.11	2.42
PI525081	0.87	0.50	0.69	1.41	1.05	0.49	0.30	0.54	1.17	1.33	2.46
PI532732	0.31	0.31	0.37	1.27	1.18	0.69	0.33	0.68	2.39	1.50	2.20
PI288522	0.55	0.44	0.67	1.41	0.98	0.64	0.36	0.46	1.26	1.38	3.00
PI381740	1.37	0.52	0.68	1.76	0.97	0.63	0.51	0.60	0.96	1.22	2.05
PI612459	0.79	0.31	0.39	1.52	1.13	0.52	0.41	0.57	1.04	1.00	1.76
CalhounGray	0.55	0.49	0.74	1.33	0.87	0.48	1.69	1.19	1.96	2.00	1.69
1410WME023	0.49	0.33	0.37	1.43	1.12	0.39	0.43	0.44	0.79	1.00	2.26
PI537300	0.92	0.25	0.29	1.70	0.91	0.83	0.51	0.77	0.75	5.73	7.45
G48	0.35	0.41	0.50	1.35	0.91	0.28	0.21	0.54	1.02	1.40	2.60
G42	0.86	0.54	0.55	1.52	1.56	0.60	0.54	0.77	2.29	7.00	9.14
ShiHongNo.2	0.43	0.77	0.88	1.37	1.16	0.52	0.32	0.44	0.78	1.00	2.26
Allsugar	0.55	0.54	0.72	1.32	0.91	0.49	0.41	0.58	1.18	1.00	1.74
G38	0.35	0.63	0.79	0.93	0.87	0.52	0.40	0.55	1.10	1.40	2.54
DaBanHongZiGua	0.44	0.33	0.50	1.44	1.24	0.47	0.44	0.58	2.31	3.00	5.21
1402WME016	0.69	0.67	0.72	1.40	1.31	0.56	0.41	0.44	1.06	1.00	2.28
SanBaiGua	0.14	0.50	0.63	0.67	0.68	0.52	0.41	0.47	1.43	1.50	3.19
CharlestonGray	0.55	1.23	1.48	1.18	1.02	0.58	0.56	0.67	1.11	1.89	2.84
Sugarlee	0.50	0.38	1.35	1.02	0.71	0.41	3.19	2.12	0.62	0.71	0.34

### 3.5. Integrated Analysis of Terminal Phenotypic Data for Drought Tolerance Evaluation

To integrate the terminal phenotypic data into a unified assessment of drought tolerance, we performed a comprehensive analysis of the DTCs for key physiological and morphological traits, alongside the  $DII_{inv}$ , where higher values indicate better drought tolerance. Correlation analysis among the twelve evaluated traits revealed complex and generally weak interrelationships (Figure 4A), with a few notable exceptions:  $DTC_{SFW}$  and  $DTC_{SDW}$  were highly positively correlated ( $r = 0.92$ ,  $p < 0.001$ ), as were  $DTC_{gs}$  and  $DTC_E$  ( $r = 0.82$ ,  $p < 0.001$ ). Root dry weight was also strongly correlated with the  $DTC_{RDW}$  and  $DTC_{RSR}$  ( $r = 0.76$ ,  $p < 0.001$ ). PCA of this dataset further confirmed the multifaceted nature of the drought response (Figure 4B). The first two PCs collectively explained 49.5% of the total variance (PC1: 31.4%; PC2: 18.1%). Accessions were widely scattered in the ordination space without forming distinct clusters. The loading vectors indicated that traits such as  $DTC_{RDW}$ ,  $DTC_{RSR}$ , and  $DTC_{ci}$  were primary contributors to PC1, whereas  $DTC_{gs}$  and  $DTC_E$  were the main drivers of PC2. This dispersed pattern of both accessions and trait vectors underscores that drought tolerance, as captured by terminal measurements, is a complex syndrome involving multiple, largely independent physiological and morphological axes. Despite the complexity at the individual trait level, a

composite evaluation using PCA and membership function analysis successfully integrated these multifaceted data into a robust comprehensive drought tolerance score (Figure 4C). The resulting ranking, based on traditional measurements, showed strong agreement with that derived from the high-throughput phenotyping platform. PI 537300, G42, and HeiShanRen were consistently identified as the top-three most tolerant accessions, whereas modern cultivars such as Charleston Gray, Sugarlee, and ShiHong No.2 were consistently ranked as the most sensitive. The comprehensive score effectively resolved the conflicting signals from individual traits into a coherent hierarchy of performance. The relationship between each accession and the full suite of traditional traits was visualized in a clustering heatmap (Figure 4D), which corroborated the comprehensive rankings. The Z-score normalized data clearly segregated the top-ranked, tolerant accessions into an upper cluster, which was generally associated with higher values for DII\_inv, DTC\_RDW, and DTC\_RSR. In contrast, the bottom-ranked, sensitive accessions formed a distinct lower cluster characterized by negative Z-scores for most traits. Hierarchical clustering analysis based on Euclidean distance further resolved the accessions into three distinct groups (Figure 4E). Cluster 1 predominantly contained highly tolerant genotypes, including the top-ranked accessions PI537300, G42, and HeiShanRen. Cluster 2 comprised a mixture of moderate and sensitive genotypes, while Cluster 3 contained the most drought-sensitive accession, Sugarlee. This clustering pattern showed good consistency with the comprehensive ranking for tolerant accessions, though some variations were observed in the classification of sensitive genotypes compared to the PCA and membership function-based D-value rankings.

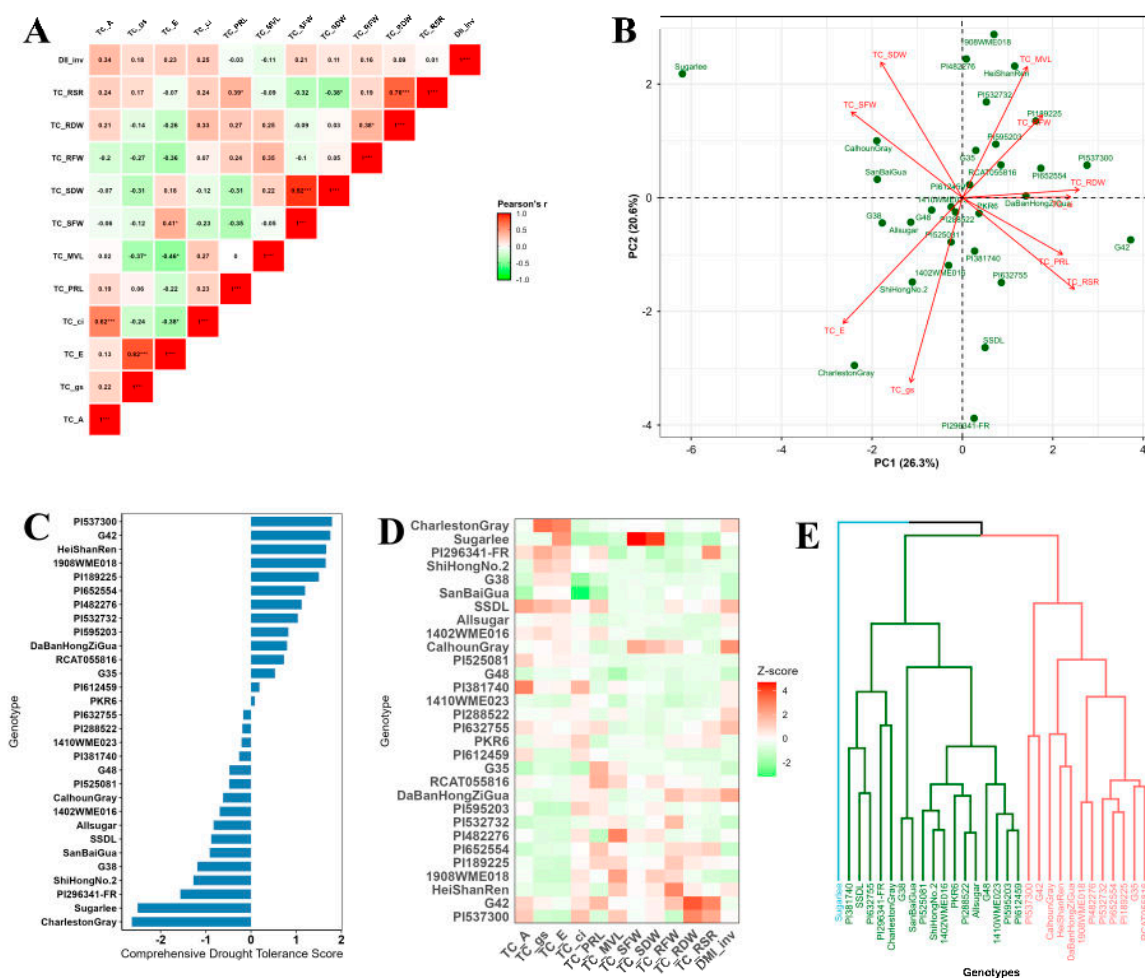


**Figure 4.** Comprehensive evaluation of drought tolerance using traditional endpoint phenotypic data. (A) Correlation matrix of DTCs and DII\_inv. Values in cells represent Pearson's correlation

coefficients ( $r$ ) with significance levels indicated as  $* p < 0.05$ ,  $*** p < 0.001$ . (B) PCA biplot showing the 30 accessions and the 12 traditional traits. The percentages of variance explained by the first and second principal components (PC1 and PC2) are 26.3% and 20.6%, respectively. (C) Drought tolerance ranking based on the comprehensive D-value derived from PCA and membership function analysis. (D) Clustered heatmap of Z-score normalized values for the 12 traditional traits across all accessions. (E) Hierarchical clustering dendrogram classifying the 30 accessions into three distinct groups: drought-tolerant (red), intermediate (green), and sensitive (blue), based on their integrated physiological strategies.

### 3.6. High Consistency Between High-Throughput Dynamic and Conventional Phenotyping

To validate the reliability of the HTP, we compared the drought tolerance rankings derived from the Plantarray system with those from conventional endpoint measurements. A highly significant positive correlation was observed between the comprehensive D-values generated by these two independent approaches ( $R = 0.941$ ,  $p < 0.001$ ; Figure 5). This strong concordance was further illustrated by representative genotypes from opposite ends of the tolerance spectrum (Figure 6). The highly tolerant accession PI 537300 maintained a high and stable TR/VPD during much of the WD phase and showed strong recovery upon WR phase (Figure 6A). In stark contrast, the highly sensitive cultivar ShiHong No.2 exhibited a rapid, drastic decline in TR/VPD shortly after drought onset, with minimal recovery. These divergent dynamic physiological responses were mirrored in terminal phenotypic data: under drought stress, PI 537300 maintained significantly higher net photosynthetic rate (A), lower stomatal conductance (gs) (Figure 6B), and greater biomass (SDW and RDW) (Figure 6C) compared to ShiHong No.2, which suffered severe inhibition in both photosynthesis and growth. The consistency between the two phenotyping approaches was further supported by hierarchical clustering analysis. Both methods effectively identified the most drought-tolerant accessions, including PI 537300, G42, and HeiShanRen, grouping them into distinct clusters, which aligned perfectly with the final classification of five tolerant (PI 537300, G42, HeiShanRen, 1908WME018, PI 189225) and four sensitive (Sugarlee, ShiHong No.2, PI 296341-FR, Charleston Gray) accessions derived from our comprehensive evaluation.

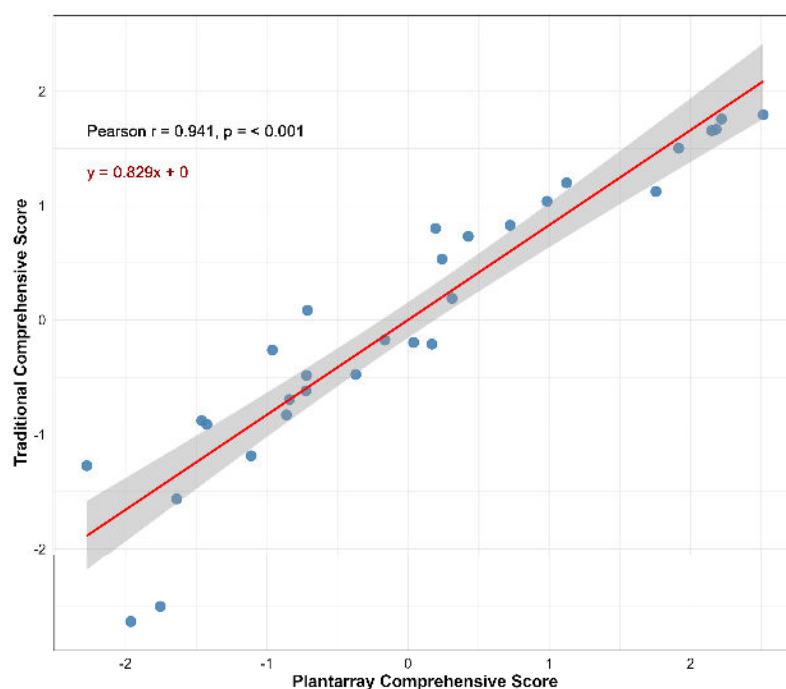


**Figure 5.** Comprehensive drought tolerance rankings from Plantarray system and conventional phenotyping are highly consistent across the 30 watermelon accessions.

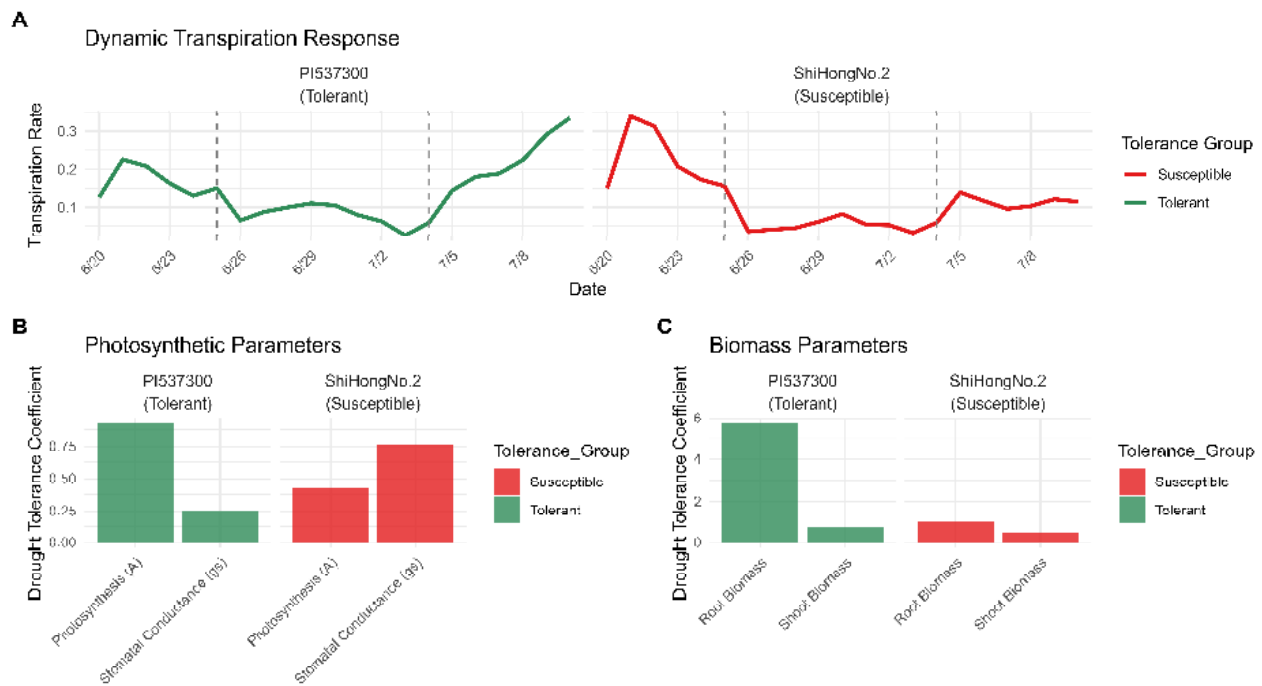


**Figure 6.** Contrasting drought responses of a highly tolerant and a highly sensitive watermelon accession. (A), Dynamics of the TR/VPD for the tolerant genotype PI 537300 and the sensitive genotype ShiHong No.2, as recorded by the Plantarray system throughout the WI, WD, and WR phases, the dotted lines indicate the initiation or termination of the WI, WD, and WR phases. (B), Comparison of key endpoint photosynthetic parameters between PI 537300 and ShiHong No.2 under WW and DS conditions: Net photosynthetic rate (A) and stomatal conductance (gs). (C), Comparison of key endpoint growth traits between PI 537300 and ShiHong No.2 under WW and DS conditions: Shoot dry weight (SDW) and root dry weight (RDW).

## 4. Discussion

Drought ranks among the most severe global meteorological disasters, with impacts intensifying under climate change. Rising global temperatures increase evaporation, expand arid areas, and impose significant constraints on agricultural production [29]. As a major abiotic stressor, drought severely impedes plant growth and development, often leading to substantial yield loss or plant mortality [30–32]. The associated losses from extreme drought events now surpass the combined losses from all pathogenic diseases [33]. The impending shortage of freshwater resources necessitates the development of crops with enhanced water use efficiency [5]. In this context, breeding and promoting drought-resistant varieties represents a highly cost-effective and efficient strategy. The success of this approach hinges on the availability of elite drought-tolerant germplasm. Therefore, establishing simple and reliable methods for identifying plant drought resistance, elucidating plant responses to drought stress, and conducting comprehensive drought tolerance evaluations are crucial for the effective screening and characterization of drought-tolerant genetic resources.

### 4.1. Diversity in Methods for Evaluating Drought Tolerance in Plants

To accurately evaluate the drought tolerance of plants, a range of methodologies has been developed, spanning from controlled laboratory simulations to field-based natural assessments. These include laboratory-based PEG-simulated drought assays [34–36], pot-based water control evaluations [37–39], and field-based natural identification [40–43]. Each method has its own advantages and disadvantages. Field identification more closely approximates actual field conditions but can be influenced by uncontrollable factors like rainfall and humidity. In contrast, the rapid induction of osmotic stress by PEG treatment

deviates from the gradual soil moisture depletion characteristic of natural drought processes in agriculture. The pot-based water control method at the seedling stage is suitable for laboratory and greenhouse environments, allowing for effective and precise water management. As such, it serves as a highly informative and practical method for assessing drought tolerance in watermelon [2]. This study employed a pot-based method to evaluate the drought tolerance of 30 watermelon accessions in a glass greenhouse (Figure 1). Alongside these varied methodologies, the assessment of drought tolerance relies on a multitude of indicators. Morphological indices include root system architecture [44], leaf characteristics [45], and plant height and biomass [2]. Physiological and biochemical indicators include the content of osmoregulatory substances (e.g., proline, soluble sugars, betaine), antioxidant enzyme activities (e.g., superoxide dismutase, peroxidase, catalase), relative electrical conductivity, and chlorophyll content [46], as well as integrated calculations for photosynthesis and water use efficiency [47]. Furthermore, the rapidly advancing field of high-throughput phenomics utilizes drones and phenotyping platforms to acquire plant image data, analyzing traits like plant height, canopy area, and leaf color for rapid assessment [48–52]. Soil moisture and plant physiological sensors also enable real-time monitoring of plant water status, facilitating drought tolerance evaluation [19,20]. Regarding watermelon germplasm, several studies have employed these methods [2], but most studies rely on traditional pot or field experiments, with no reported application of high-throughput phenomics for screening drought tolerance in watermelon to date.

#### *4.2. Comprehensive Multi-Indicator Evaluation Strategies for Complex Drought Tolerance Traits*

Drought tolerance is a complex polygenic trait, and a single indicator cannot fully reflect a plant's drought tolerance capacity. Therefore, comprehensive evaluation using multiple indicators is essential. An increasing number of studies are shifting from single-trait reliance to joint multi-indicator analysis, with membership function values and comprehensive evaluation D-values being the most widely used methods [28]. These computational methods effectively integrate information from multiple, potentially intercorrelated, physiological and morphological indicators. Zhang et al. (2021) [53] calculated membership function values for six indicators to evaluate drought tolerance in German iris. Li et al. (2023) [54] transformed 13 physiological and biochemical indicators into four composite indicators via PCA and evaluated lettuce drought tolerance using three methods (D-value, CDC, WDC). Ren et al. (2025) [2] conducted correlation analysis and PCA on 27 traits, computed membership function values and D-values, and classified 13 watermelon varieties through cluster analysis. Following a comprehensive evaluation, they identified one highly tolerant and six tolerant germplasms. This integrated approach of PCA, D-value, and cluster analysis offers a robust and widely adopted framework for comprehensive stress resistance evaluation in plants. By relying on computational data, these methods reduce subjective judgment influence, ensuring objectivity and repeatability. Consequently, membership function values and D-values provide scientific, efficient, and objective technical means for evaluating plant drought tolerance and are widely applied in crop breeding and resource screening. This study adopted these methods to assess drought tolerance in watermelon.

#### *4.3. High-Throughput Phenotyping Systems Demonstrate Significant Potential in Plant Drought Tolerance Evaluation*

Plants perceive and respond to drought as a dynamic process, wherein stress severity intensifies with declining soil moisture but can be alleviated upon rehydration. Consequently, relying solely on endpoint, destructive data for assessing drought tolerance presents significant limitations [2,16,17]. Phenomics has emerged to address this gap by enabling real-time, dynamic, and continuous monitoring of plant responses. This ap-

proach captures key processes throughout the drought cycle: active acclimation during water depletion, tolerance under extreme stress, and recovery capacity following rewatering. While both spectral and physiology-based phenotyping technologies have been widely reported [17,48], this study specifically pioneers the validation of the Plantarray system for watermelon. Our results demonstrate high consistency ( $r = 0.97$ ) with conventional methods in ranking 30 accessions. Crucially, dynamic TR monitoring under VPD uncovered accession-specific resilience mechanisms that were invisible to conventional metrics (Figure 2), underscoring the system's superior resolving power. Correlation analysis among four dynamic physiological indices—TMR, CTR, WUEI, and TRR—revealed distinct drought response strategies among the accessions. Strong positive correlations between TMR, CTR, and WUEI defined a “maintenance-type” strategy, employed by accessions such as PI 537300 and G42, which sustained higher transpiration and photosynthesis for longer during drought while improving water-use efficiency. In contrast, TRR showed weak correlations with the other indices, defining an independent “recovery-type” strategy. A representative example is PI 532732, which exhibited superior post-stress recovery ( $TRR > 1.2$ ) without possessing the strongest maintenance capacity. This strategic divergence was further illustrated by a clear separation along PC1 (maintenance capacity) and PC2 (recovery capacity) in a PCA, highlighting the trade-offs between these strategic axes. Such nuanced divergence is exceptionally difficult to resolve using conventional endpoint data, where final biomass or survival rate often represents a consolidated outcome of potentially different underlying strategies. Although phenomics offers significant advantages by minimizing manual operation and providing continuous monitoring, its widespread application is currently constrained by high technical costs. Nevertheless, given its unparalleled capacity to deconstruct complex traits, we anticipate that high-throughput physio-phenomics will become an indispensable tool for crop phenotype identification, particularly for intricate agronomic traits like drought tolerance.

#### 4.4. Identification of Elite Germplasm and Its Breeding Value

This study successfully identified several extremely drought-tolerant accessions, with the wild species PI 537300 and the cultivated variety G42 performing most prominently. The superior drought tolerance of PI 537300 is consistent with the known resilience of wild progenitors and represents a valuable resource for introducing novel allelic diversity into cultivated watermelon, a strategy pivotal for enhancing stress resilience in other cucurbit crops [54]. Particularly valuable is the identification of G42 as a highly tolerant genotype within the cultivated gene pool. It performed excellently not only in dynamic physiological indices but also ranked highly in traditional measurements of biomass, photosynthesis, and root traits. The discovery of G42 demonstrates that significant and unexploited genetic variation for complex traits like drought tolerance persists within elite cultivated germplasm, and its utilization through intraspecific hybridization would be more direct and efficient, avoiding the linkage drag commonly associated with wild-species introgression [55]. Conversely, the identified extremely sensitive materials (e.g., ShiHong No.2, Sugarlee) serve as ideal negative controls for comparative transcriptomics and for establishing reliable phenotyping protocols in breeding populations [56]. These extreme materials, with their well-characterized physiological responses, collectively form a core germplasm set for subsequent multi-omics studies to dissect the molecular basis of drought tolerance [11], laying a solid foundation for the cloning of causal genes and their deployment in marker-assisted selection breeding programs.

In summary, this study establishes a high-throughput phenotyping framework for watermelon drought tolerance by validating the efficient Plantarray platform. This approach uncovered distinct physiological drought resistance strategies and identified core

germplasm. The existence of these strategy-specific materials provides breeders with flexible tools to develop targeted cultivars for different agroecological conditions. The work provides both novel physiological perspectives and practical genetic tools to accelerate the breeding of drought-resilient watermelon cultivars.

**Supplementary Materials:** The following supporting information can be downloaded at: <https://www.mdpi.com/article/10.3390/horticulturae11111374/s1>, Table S1: Environmental parameters exported from the Plantarray system; Table S2: The Information of 30 watermelon accessions in the Plantarray system experiment; Table S3: System unit weight parameters exported from the Plantarray system during the experiment; Table S4: Variation in drought injury index among 30 watermelon accessions under drought stress in the Phenotray system; Table S5: Variation in drought injury index among 30 watermelon accessions under drought stress in the traditional method; Table S6: Transpiration rate (TR) parameters per unit exported from the Plantarray system during the experiment; Table S7: Soil water content (VWC) parameters per unit exported from the Plantarray system during the experiment; Table S8: Photosynthesis and growth parameters of the WW group in the conventional method experiment; Table S9: Photosynthesis and growth parameters of the DS group in the conventional method experiment.

**Author Contributions:** Conceptualization, X.W. and Y.S.; methodology, R.C. and Y.S.; software, R.C. and S.Z.; validation, B.X. and C.J.; formal analysis, X.L. and Y.T.; investigation, X.S. and W.X.; writing—original draft preparation, R.C.; writing—review and editing, X.W.; funding acquisition, R.C., Y.S. and X.W. All authors have read and agreed to the published version of the manuscript.

**Funding:** This research was funded by the Huai'an Natural Science Research Project/Research and Development Fund Project of Huai'an Academy of Agricultural Sciences (HABL202228), Doctoral Research Initiation Fund of Huai'an Academy of Agricultural Sciences (0012023011B), China Agriculture Research System of MOF and MARA (CARS-25), the Seed Industry Vitalization Research Projects of Jiangsu Province (JBGS [2021]072), and Jiangsu Agriculture Science and Technology Innovation Fund (CX(24)1027).

**Data Availability Statement:** The original contributions presented in this study are included in the article. Further inquiries can be directed to the authors.

**Acknowledgments:** The authors express gratitude for the invaluable support received during the research process. We greatly appreciate the watermelon germplasm provided by the Crop Breeding Platform of the Peking University Institute of Advanced Ag Sciences. Additionally, we would like to extend our sincere thanks to Pei Xu and his team from China Jiliang University for their expert guidance and technical support in the application of the Plantarray system.

**Conflicts of Interest:** The authors declare no conflicts of interest.

## Abbreviations

The following abbreviations are used in this manuscript:

WUE	Water Use Efficiency
Tair	Air Temperature
PAR	Photosynthetically Active Radiation
RH	Relative Humidity
VPD	Vapor Pressure Deficit
Tsoil	Soil Temperature
WI	Well Irrigated
WD	Progressive Water Deficit
WR	water recovery
DS	Drought Stress
WW	Well Watered
PG	Plant Growth

TR	Transpiration Rate
A	Net Photosynthetic Rate
Ci	Intercellular CO <sub>2</sub> Concentration
gs	Stomatal Conductance
VL	Vine Length
RL	Root Length
SFW	Shoot Fresh Weight
RFW	Root Fresh Weight
SDW	Shoot Dry Weight
RSR	Root Shoot Ratio
TMR	Transpiration Maintenance Ratio
CTR	Cumulative Transpiration Ratio
WUEI	Water Use Efficiency Increase Ratio
TRR	Transpiration Recovery Ratio
DTC	Drought Tolerance Coefficient
PCA	Principal Component Analysis
D-value	Drought Tolerance value

## References

- Sun, H.; Zhang, J.; Liao, S.; Guo, S.; Zhou, Z.; Zhao, X.; Wu, S.; Zhao, J.; Gong, G.; Wang, J.; et al. Population-level super-genome reveals genome evolution and empowers precision breeding in watermelon. *bioRxiv* **2025**. [\[CrossRef\]](#)
- Ren, K.; Tang, T.; Kong, W.; Su, Y.; Wang, Y.; Cheng, H.; Yang, Y.; Zhao, X. Response of watermelon to drought stress and its drought-resistance evaluation. *Plants* **2025**, *14*, 1289. [\[CrossRef\]](#) [\[PubMed\]](#)
- Márkus, R.; Czige, S.; Zana, B.; Somogyi, B.; Urbán, P.; Kutyáncsánin, D.; Helfrich, P.; Stranczinger, S. Drought and salt stressors alter NAC and WRKY gene expression profiles in grafted *Citrullus lanatus*. *Plant Mol. Biol. Report.* **2025**, *43*, 1576–1587. [\[CrossRef\]](#)
- Li, H.; Mo, Y.; Cui, Q.; Yang, X.; Guo, Y.; Yang, Y.; Wei, C.; Zhang, Y.; Ma, J.; Zhang, X. Transcriptomic and physiological analyses reveal drought adaptation strategies in drought-tolerant and -susceptible watermelon genotypes. *Plant Sci.* **2019**, *278*, 32–43. [\[CrossRef\]](#)
- Gupta, A.; Rico-Medina, A.; Caño-Delgado, A.I. The physiology of plant responses to drought. *Science* **2020**, *368*, 266–269. [\[CrossRef\]](#)
- Wang, C.; Li, Z.; Chen, Y.; Yang, O.; Zhao, H.; Zhu, J.; Wang, J.; Zhao, Y. Characteristic changes in compound drought and heatwave events under climate change. *Atmos. Res.* **2024**, *35*, 107440. [\[CrossRef\]](#)
- Cook, B.I.; Smerdon, J.E.; Mankin, J.S.; Marvel, K.; Williams, A.P.; Anchukaitis, K.J. Twenty-first century drought projections in the CMIP6 forcing scenarios. *Earth's Future* **2020**, *8*, e2019EF001461. [\[CrossRef\]](#)
- Huang, J.; Yu, H.; Guan, X.; Wang, G.; Guo, R. Accelerated dryland expansion under climate change. *Nat. Clim. Change* **2016**, *6*, 166–171. [\[CrossRef\]](#)
- Cao, Y.; Yang, W.; Ma, J.; Cheng, Z.; Zhang, X.; Liu, X.; Wu, X.; Zhang, J. An Integrated framework for drought stress in plants. *Int. J. Mol. Sci.* **2024**, *25*, 9347. [\[CrossRef\]](#)
- Hura, T.; Hura, K.; Ostrowska, A. Drought-stress induced physiological and molecular changes in plants. *Int. J. Mol. Sci.* **2022**, *23*, 4698. [\[CrossRef\]](#)
- Zhang, H.; Zhu, J.; Gong, Z.; Zhu, J. Abiotic stress responses in plants. *Nat. Rev. Genet.* **2022**, *23*, 104–119. [\[CrossRef\]](#)
- Shirani Rad, A.H.; Abbasian, A. Evaluation of drought tolerance in rapeseed genotypes under non stress and drought stress conditions. *Not. Bot. Horti Agrobot. Cluj-Napoca* **2011**, *39*, 164–171. [\[CrossRef\]](#)
- Naghavi, M.R.; Pour Aboughadareh, A.; Khalili, M. Evaluation of drought tolerance indices for screening some of corn (*Zea mays* L.) cultivars under environmental conditions. *Not. Sci. Biol.* **2013**, *5*, 388–393. [\[CrossRef\]](#)
- Fahlgren, N.; Gehan, M.A.; Baxter, I. Lights, camera, action: High-throughput plant phenotyping is ready for a close-up. *Curr. Opin. Plant Biol.* **2015**, *24*, 93–99. [\[CrossRef\]](#) [\[PubMed\]](#)
- Gosa, S.C.; Lupo, Y.; Moshelion, M. Quantitative and comparative analysis of whole-plant performance for functional physiological traits phenotyping: New tools to support pre-breeding and plant stress physiology studies. *Plant Sci.* **2019**, *282*, 49–59. [\[CrossRef\]](#)
- Halperin, O.; Gebremedhin, A.; Wallach, R.; Moshelion, M. High-throughput physiological phenotyping and screening system for the characterization of plant-environment interactions. *Plant J.* **2017**, *89*, 839–850. [\[CrossRef\]](#)

17. Dalal, A.; Bourstein, R.; Haish, N.; Shenhar, I.; Wallach, R.; Moshelion, M. Dynamic physiological phenotyping of drought-stressed pepper plants treated with “productivity-enhancing” and “survivability-enhancing” biostimulants. *Front. Plant Sci.* **2019**, *10*, 905. [[CrossRef](#)]
18. Li, Y.; Wu, X.; Xu, W.; Sun, Y.; Wang, Y.; Li, G.; Xu, P. High-throughput physiology-based stress response phenotyping: Advantages, applications and prospective in horticultural plants. *Hortic. Plant J.* **2021**, *7*, 181–187. [[CrossRef](#)]
19. Mika, F.; Ziv, A.; David, W. Cytokinin activity increases stomatal density and transpiration rate in tomato. *J. Exp. Bot.* **2016**, *67*, 6351–6362. [[CrossRef](#)]
20. Fang, P.; Sun, T.; Pandey, A.K.; Jiang, L.; Wu, X.; Hu, Y.; Cheng, S.; Li, M.; Xu, P. Understanding water conservation vs. profligation traits in vegetable legumes through a physio-transcriptomic-functional approach. *Hortic. Res.* **2023**, *10*, uhac287. [[CrossRef](#)]
21. Paul, M.; Dalal, A.; Jääskeläinen, M.; Moshelion, M.; Schulman, H. Precision phenotyping of a barley diversity set reveals distinct drought response strategies. *Front. Plant Sci.* **2024**, *15*, 1393991. [[CrossRef](#)]
22. Sun, T.; Cheng, R.; Jiang, R.; Liu, Y.; Sun, Y.D.; Wang, Z.Y.; Fang, P.P.; Wu, X.Y.; Ning, K.; Xu, P. Combining functional physiological phenotyping and simulation model to estimate dynamic water use efficiency and infer transpiration sensitivity traits. *Eur. J. Agron.* **2023**, *150*, 126955. [[CrossRef](#)]
23. He, Y.P.; Yin, L.J.; Ding, X.L.; Wang, C.X.; Hou, Y.J.; Ma, H.Y.; Yu, R.; Yue, Z.; Yang, J.Q.; Zhang, X.; et al. Identification and screening of drought resistance indexes of 25 watermelon germplasm at seedling stage. *J. Northwest AF Univ. (Nat. Sci. Ed.)* **2023**, *51*, 49–59. [[CrossRef](#)]
24. Sade, N.; Gebretsadik, M.; Seligmann, R.; Schwartz, A.; Wallach, R.; Moshelion, M. The role of tobacco Aquaporin1 in improving water use efficiency, hydraulic conductivity, and yield production under salt stress. *Plant Physiol.* **2014**, *165*, 512–523. [[CrossRef](#)]
25. Mohammadi, R. Efficiency of yield-based drought tolerance indices to identify tolerant genotypes in durum wheat. *Euphytica* **2016**, *211*, 71–89. [[CrossRef](#)]
26. Jolliffe, I.T.; Cadima, J. Principal component analysis: A review and recent developments. *Philos. Trans. R. Soc. A Math. Phys. Eng. Sci.* **2016**, *374*, 20150202. [[CrossRef](#)]
27. Du, W.; Zhang, F.L.; Zhang, L.; Hu, M.; Tian, H.; Ying, H.; Ding, S.; Dan, X. Comprehensive evaluation and screening of drought resistance in maize at germination and seedling stages. *Front. Plant Sci.* **2025**, *16*, 1672228. [[CrossRef](#)]
28. Liang, Z.; Pei, K.; Zhang, H.; Lai, X.; Meng, Y.; Jia, M.; Cao, D.; Zhang, C.; Song, Z.; Duan, J. A comprehensive evaluation of drought resistance in *Hemerocallis fulva* L. using membership function and principal component analysis. *Sci. Rep.* **2025**, *15*, 34812. [[CrossRef](#)]
29. Wang, W.; Wang, J.; Shao, J.; Wu, B.; Lin, H. The spatiotemporal variation characteristics and impacts of summer heatwaves, droughts, and compound drought and heatwave events in Jiangsu Province, China. *Water* **2024**, *16*, 89. [[CrossRef](#)]
30. Nawaz, M.; Shabbir, S.; Nazir, M.M.; Anas, M.; Farooq, M.; Xu, H.; Yang, W.; Ahmad, P.; Li, L.; Wang, Z. Adaptive strategies of carpet grass to drought: Insights from physiological and antioxidant responses. *J. Plant Growth Regul.* **2025**. [[CrossRef](#)]
31. Mourad, K.; Othman, Y.I.M.; Kandeel, D.M.; Abdelghany, M. Assessing the drought tolerance of some sesame genotypes using agro-morphological, physiological, and drought tolerance indices. *BMC Plant Biol.* **2025**, *25*, 352. [[CrossRef](#)]
32. Mukherjee, A.; Dwivedi, S.; Bhagavatula, L.; Datta, S. Integration of light and ABA signaling pathways to combat drought stress in plants. *Plant Cell Rep.* **2023**, *42*, 829–841. [[CrossRef](#)]
33. Gong, Z.Z.; Xiong, L.M.; Shi, H.Z.; Yang, S.H.; Herrera-Estrella, L.R.; Xu, G.H.; Chao, D.Y.; Li, J.R.; Wang, P.Y.; Qin, F.; et al. Plant abiotic stress response and nutrient use efficiency. *Sci. China Life Sci.* **2020**, *63*, 635–674. [[CrossRef](#)]
34. Badr, A.; El-Shazly, H.H.; Tarawneh, R.A.; Börner, A. Screening for drought tolerance in maize (*Zea mays* L.) germplasm using germination and seedling traits under simulated drought conditions. *Plants* **2020**, *9*, 565. [[CrossRef](#)] [[PubMed](#)]
35. Wei, X.; Cang, B.; Yu, K.; Li, W.; Tian, P.; Han, X.; Wang, G.; Di, Y.; Wu, Z.; Yang, M. Physiological characterization of drought responses and screening of rice varieties under dry cultivation. *Agronomy* **2022**, *12*, 2849. [[CrossRef](#)]
36. Chen, D.; Wang, S.; Cao, B.; Cao, D.; Leng, G.; Li, H.; Yin, L.; Shan, L.; Deng, X. Genotypic variation in growth and physiological response to drought stress and re-watering reveals the critical role of recovery in drought adaptation in maize seedlings. *Front. Plant Sci.* **2016**, *6*, 1241. [[CrossRef](#)] [[PubMed](#)]
37. Wang, Y.; Huang, Q.; Liu, L.; Li, H.; Wang, X.; Si, A.; Yu, Y. Screening and comprehensive evaluation of drought resistance in cotton germplasm resources at the germination stage. *Plants* **2025**, *14*, 2191. [[CrossRef](#)]
38. Zhao, X.; Liu, Z.; Li, H.; Zhang, Y.; Yu, L.; Qi, X.; Gao, H.; Li, Y.; Qiu, L. Identification of drought-tolerance genes in the germination stage of soybean. *Biology* **2022**, *11*, 1812. [[CrossRef](#)] [[PubMed](#)]
39. Mohi-Ud-Din, M.; Hossain, M.A.; Rohman, M.M.; Uddin, M.N.; Haque, M.S.; Ahmed, J.U.; Hossain, A.; Hassan, M.M.; Mostofa, M.G. Multivariate analysis of morpho-physiological traits reveals differential drought tolerance potential of bread wheat genotypes at the seedling stage. *Plants* **2021**, *10*, 879. [[CrossRef](#)]
40. Bao, X.; Hou, X.; Duan, W.; Yin, B.; Ren, J.; Wang, Y.; Liu, X.; Gu, L.; Zhen, W. Screening and evaluation of drought resistance traits of winter wheat in the North China Plain. *Front. Plant Sci.* **2023**, *14*, 1194759. [[CrossRef](#)]

41. Martínez, I.; Muñoz, M.; Acuña, I.; Uribe, M. Evaluating the drought tolerance of seven potato varieties on volcanic ash soils in a medium-term trial. *Front. Plant Sci.* **2021**, *12*, 693060. [[CrossRef](#)]
42. Shojaei, S.H.; Mostafavi, K.; Omrani, A.; Illés, Á.; Bojtor, C.; Omrani, S.; Mousavi, S.M.N.; Nagy, J. Comparison of maize genotypes using drought-tolerance indices and graphical analysis under normal and humidity stress conditions. *Plants* **2022**, *11*, 942. [[CrossRef](#)]
43. Tiwari, P.N.; Tiwari, S.; Sapre, S.; Tripathi, N.; Payasi, D.K.; Singh, M.; Thakur, S.; Sharma, M.; Tiwari, S.; Tripathi, M.K. Prioritization of physio-biochemical selection indices and yield-attributing traits toward the acquisition of drought tolerance in chickpea (*Cicer arietinum* L.). *Plants* **2023**, *12*, 3175. [[CrossRef](#)]
44. Mandizvo, T.; Odindo, A.O.; Mashilo, J.; Sibiya, J.; Beck-Pay, S.L. Phenotypic variability of root system architecture traits for drought tolerance among accessions of citron watermelon (*Citrullus lanatus* var. *citroides* (L.H. Bailey)). *Plants* **2022**, *11*, 2522. [[CrossRef](#)]
45. Sadeghi Seresht, E.; Karimi, H.R.; Malekzadeh, K.; Mirdehghan, S.H.; Mirik, A.A.M.; Jomeyazdiyan, M.S. Evaluation of morphological and physiological traits as indicators of drought tolerance in twelve pomegranate cultivars (*Punica granatum* L.). *Russ. J. Plant Physiol.* **2025**, *72*, 131. [[CrossRef](#)]
46. Jin, Y.; Zhao, X.; Liu, W.; Liang, G.; Zhang, Y. Germplasm resources and drought resistance evaluation of Siberian wildrye (*Elymus sibiricus* L.) in the Tibetan Plateau. *Braz. J. Bot.* **2023**, *46*, 743–756. [[CrossRef](#)]
47. Takudzwa, M.; Alfred, O.O.; Jacob, M.; Lembe, S.M. Drought tolerance assessment of citron watermelon (*Citrullus lanatus* var. *citroides* (L.H. Bailey) Mansf. ex Greb.) accessions based on morphological and physiological traits. *Plant Physiol. Biochem.* **2022**, *180*, 106–123. [[CrossRef](#)] [[PubMed](#)]
48. Wonneberger, R.; D’Auria, C.J.; Neumann, K.; Hansen, P.B.; Dieseth, J.A.; Nielsen, L.K.; Niemelä, T.; Odilbekov, F.; Novakazi, F.; Bengtsson, T.; et al. Integrating metabolomics and high-throughput phenotyping to elucidate metabolic and phenotypic responses to early-season drought stress in Nordic spring wheat. *BMC Plant Biol.* **2025**, *25*, 987. [[CrossRef](#)] [[PubMed](#)]
49. Anand, S.L.; Visakh, R.; Nalishma, R.; Sah, R.P.; Beena, R. High-throughput phenomics in elucidating drought stress responses in rice (*Oryza sativa* L.). *J. Plant Biochem. Biotechnol.* **2024**, *34*, 119–132. [[CrossRef](#)]
50. Zhang, J.; Maleski, J.; Ashrafi, H.; Spencer, J.A.; Chu, Y. Open-source high-throughput phenotyping for blueberry yield and maturity prediction across environments: Neural Network Model and Labeled Dataset for Breeders. *Horticulturae* **2024**, *10*, 1332. [[CrossRef](#)]
51. Herzog, K.; Kicherer, A.; Malagol, N.; Trapp, O.; Töpfer, R. High-throughput phenotyping in grapevine breeding research: Technologies and applications. *OENO One* **2025**, *59*, 3. [[CrossRef](#)]
52. Sneha-Priya, P.R.; Sudhir, K.; Jiayin, P.; Chellapilla, B.; Pal, M.; Millar, A.H.; Siddique, K.H. High-throughput phenotyping for terminal drought stress in chickpea (*Cicer arietinum* L.). *Plant Stress* **2024**, *11*, 100386. [[CrossRef](#)]
53. Zhang, J.; Huang, D.; Zhao, X.; Zhang, M. Evaluation of drought resistance and transcriptome analysis for the identification of drought-responsive genes in *Iris germanica*. *Sci. Rep.* **2021**, *11*, 16308. [[CrossRef](#)]
54. Li, J.; Abbas, K.; Wang, L.; Gong, B.; Hou, S.; Wang, W.; Dai, B.; Xia, H.; Wu, X.; Lü, G.; et al. Drought resistance index screening and evaluation of lettuce under water deficit conditions on the basis of morphological and physiological differences. *Front. Plant Sci.* **2023**, *14*, 1228084. [[CrossRef](#)] [[PubMed](#)]
55. Bai, Y.; Bai, P.L. Domestication and breeding of tomatoes: What have we gained and what can we gain in the future? *Ann. Bot.* **2007**, *100*, 1085–1094. [[CrossRef](#)] [[PubMed](#)]
56. Clevenger, J.; Chavarro, C.; Pearl, S.A.; Ozias-Akins, P.; Jackson, S.A. Single nucleotide polymorphism identification in polyploids: A review, example, and recommendations. *Mol. Plant* **2015**, *8*, 831–846. [[CrossRef](#)] [[PubMed](#)]

**Disclaimer/Publisher’s Note:** The statements, opinions and data contained in all publications are solely those of the individual author(s) and contributor(s) and not of MDPI and/or the editor(s). MDPI and/or the editor(s) disclaim responsibility for any injury to people or property resulting from any ideas, methods, instructions or products referred to in the content.